Fractional-Order Modeling of Arterial Compliance in Vascular Aging: A Computational Biomechanical Approach for Investigating Cardiovascular Dynamics

Mohamed A. Bahloul [ID], Yasser Aboelkassem [ID], Zehor Belkhatir [ID],
and Taous-Meriem Laleg-Kirati [ID], *Senior Member, IEEE*

Abstract—Goal: The goal of this study is to investigate the application of fractional-order calculus in modeling arterial compliance in human vascular aging. *Methods:* A novel fractional-order modified arterial Windkessel model that incorporates a fractional-order capacitor (FOC) element is proposed to capture the complex and frequency-dependent properties of arterial compliance. The model's performance is evaluated by verifying it using data collected from three different human subjects, with a specific focus on aortic pressure and flow rates. *Results:* The results show that the FOC model accurately captures the dynamics of arterial compliance, providing a flexible means to estimate central blood pressure distribution and arterial stiffness. *Conclusions:* This study demonstrates the potential of fractional-order calculus in advancing the modeling and characterization of arterial compliance in human vascular aging. The proposed FOC model can improve our understanding of the physiological changes in arterial compliance associated with aging and help to identify potential interventions for age-related cardiovascular diseases.

Mohamed A. Bahloul is with the Electrical Engineering Department, College of Engineering, Alfaisal University, Riyadh 11533, Saudi Arabia (e-mail: mbahloul@alfaisal.edu).

Yasser Aboelkassem is with the College of Innovation and Technology, University of Michigan, Flint, MI 48502 USA, and also with Michigan Institute for Data Science, University of Michigan, Ann Arbor, MI 48109 USA (e-mail: yassera@umich.edu).

Zehor Belkhatir is with the Digital Health & Biomedical Engineering Group, School of Electronics and Computer Science, University of Southampton, SO17 1BJ Southampton, U.K. (e-mail: z.belkhatir@soton.ac.uk).

Taous-Meriem Laleg-Kirati is with the Computer, Electrical and Mathematical Sciences and Engineering, King Abdullah University of Science and Technology (KAUST), Makkah 23955, Saudi Arabia, and also with the National Institute for Research in Digital Science and Technology, 78150 Paris-Saclay, France (e-mail: taousmeriem.laleg@kaust.edu.sa).

Digital Object Identifier 10.1109/OJEMB.2023.3343083

Index Terms—Fractional calculus, fractional-order capacitor, vascular compliance, aortic input impedance.

Impact Statement—Fractional-order calculus improves arterial compliance modeling for human vascular aging. Our model accurately estimates blood pressure distribution and stiffness, advancing the understanding of cardiovascular disease.

I. INTRODUCTION

VASCULAR compliance pertains to an arterial vessel's ability to accommodate blood volume changes. This property characterizes the vascular wall's capacity to flexibly expand and augment vessel volume in response to an elevation in transmural pressure, or inversely, its propensity to withstand compression and revert to its original shape [1], [2], [3]. Recent decades have witnessed a marked interest in comprehending the interplay between variations in arterial compliance and cardiovascular diseases. The clinical significance of vascular compliance arises from its pivotal role in pulsatile hemodynamics. Consequently, numerous clinical and experimental research endeavors have emerged to quantify vascular compliance, leading to the development of diverse surrogate markers for arterial compliance [4], [5]. In this context, a spectrum of linear and non-linear computational techniques for assessing vascular compliance has been presented in the literature [6], [7]. These include: 1) The Time Decay method, also recognized as the linear Windkessel model compliance [8], [9], 2) The Area method [10], 3) The Stroke Volume over Pulse Pressure method [11], [12], 4) The Exponential method, and more recently, 5) The compliance-pressure loop approach [13], [14].

Functionally, arterial compliance manifests through the relationship between fluctuations in stored blood volume and corresponding alterations in input blood pressure. Analogously, the concept of total arterial compliance has been introduced as the summation of compliance components across the entire arterial system. Thus, the aggregate compliance quantifies the global arterial capacity for blood storage and is calculated by

dividing the variation in blood volume throughout the arterial system by the fluctuation in systemic input pressure. However, this ratio is influenced not solely by total arterial compliance but also encompasses factors such as pulse wave reflection. It accurately represents total compliance only at low frequencies. Therefore, the concept of dynamic arterial compliance–alternatively termed apparent compliance–was introduced by Quick et al. [2] to elucidate the accurate estimation of true total compliance through the transfer function connecting blood volume and input pressure [15]. This concept addresses the question of whether conventional methods of estimating arterial compliance fall short of determining actual arterial compliance. Prior to the advent of the "apparent compliance" notion, the transfer function associating blood volume with systemic input pressure was considered constant, akin to the capacitance of an ideal capacitor in electrical analog modeling. This assumption hinged on the Windkessel concept embraced by lumped-element modeling principles. Limitations of this assumption surfaced in compliance estimation methods, resulting in inaccurate evaluations of true arterial compliance [16]. The distributed nature of vascular compliance and resistance within the arterial network underscores the frequency-dependent nature of the blood volume/input pressure relationship [2]. This translates to a temporal delay between arterial blood volume and input pressure. Over the past decades, clinical studies have underscored the necessity of introducing apparent compliance to extract total compliance. Consequently, a novel lumped-parameter modeling framework, considering the intricate frequency-dependent properties of apparent arterial compliance, was proposed [17]. These models posit that the arterial wall possesses viscoelastic properties as opposed to pure elasticity. The Voigt cell model (comprising a resistor in series with a capacitor) emerged as a suitable candidate for representing total arterial compliance. The resistor embodies viscous losses linked to arterial wall motion, while the capacitor symbolizes static artery compliance. The synergy between these resistor and capacitor elements gives rise to complex, frequency-dependent compliance. However, the Voigt model's configuration inadequately captures arterial viscoelasticity, as it fails to account for stress-relaxation experiments [18]. To address this gap, the viscoelastic representation's order was augmented by introducing additional viscous and elastic interconnected elements [17]. This higher-order configuration yields heightened accuracy at the expense of complexity, primarily attributed to an extensive set of unknown parameters, thereby presenting a challenge. Indeed, higher-order models necessitate identifying a larger number of parameters, whereas the available real-world data remains limited and insufficient. Additionally, it is recognized that reduced-order models are desirable for their simplicity and ease of exploration, [3], [19].

In the last decades, non-integer differentiation, the so-called fractional-order differential calculus, became a popular tool for characterizing real-world physical systems and complex behaviors from various fields such as biology, control, electronics, and economics [20], [21]. The long-memory and spatial dependence phenomena inherent to the fractional-order systems present unique and attractive peculiarities that raise exciting opportunities to represent complex phenomena that represent power-law behavior accurately. Regarding cardiovascular modeling,

the power-law behavior has been demonstrated in describing human soft tissues' visco-elasticity and characterizing the elastic vascular arteries. The in-vivo and in-vitro experimental studies have pointed out that fractional-order calculus-based approaches are more decent to represent the hemodynamic precisely; the viscoelasticity properties of soft collagenous tissues in the vascular bed; the aortic blood rate [22], [23], [24]; red blood cell (RBC) membrane mechanical properties [25] and the heart valve cusp [23], [26], [27], [28]. In addition, recently, we developed novel fractional-order arterial Windkessel representations, [29], [30], [31]. The proposed framework takes advantage of the relevant fractional-order calculus tools. Basically, the fractional-order Windkessel representations are similar to the well-known Windkessel configurations; however, instead of representing the arterial compliance with an ideal capacitor which is purely a storage element, we investigate the use of the fractional-order element, namely the fractional-order capacitor, [32]. Our elemental investigations in the frequency domain showed that the proposed models accurately reconstruct the arterial impedance and solve the hemodynamic inverse problem by estimating the different vascular biomechanics determinants. Moreover, a clear association between the central hemodynamic parameters and the fractional differentiation order (α) has been observed. In this context, fractional orders have been employed to describe and control the transition between viscosity and elasticity, [33], [34].

In this paper, we present five fractional-order model representations to describe the apparent vascular compliance by representing the active relationship between blood pressure and volume. Each configuration incorporates a fractional-order capacitor element (FOC) to lump the apparent arterial compliance's complex and frequency dependence properties. FOC combines both resistive and capacitive attributes within a unified component, controlled through the fractional differentiation order, α. Besides, the equivalent capacitance of FOC is inherently frequency-dependent, compassing the complex properties using only a few numbers of parameters. To show the added value of the fractional-order element, we compare the proposed models to the standard integer-order models. Moreover, the simplest fractional-order representation of the proposed paradigm has been combined into a global arterial lumped parameter representation forming a novel fractional-order modified arterial Windkessel. All models have been applied and validated using aortic pressure and flow rate data acquired from three human subjects at different ages, namely 28, 52, and 68 years. The results show the aptitude and flexibility of the fractional-order models in fitting different apparent compliance dynamics and central blood pressure measurements while maintaining a low model complexity. Fig. 1 illustrates in a schematic manner the general framework for fractional-order modeling of the apparent vascular compliance and the arterial system.

II. PRELIMINARIES

A. Apparent Compliance

The apparent compliance, C_{app}, refers to the arterial bed's capacity to store blood dynamically. Functionally, it corresponds
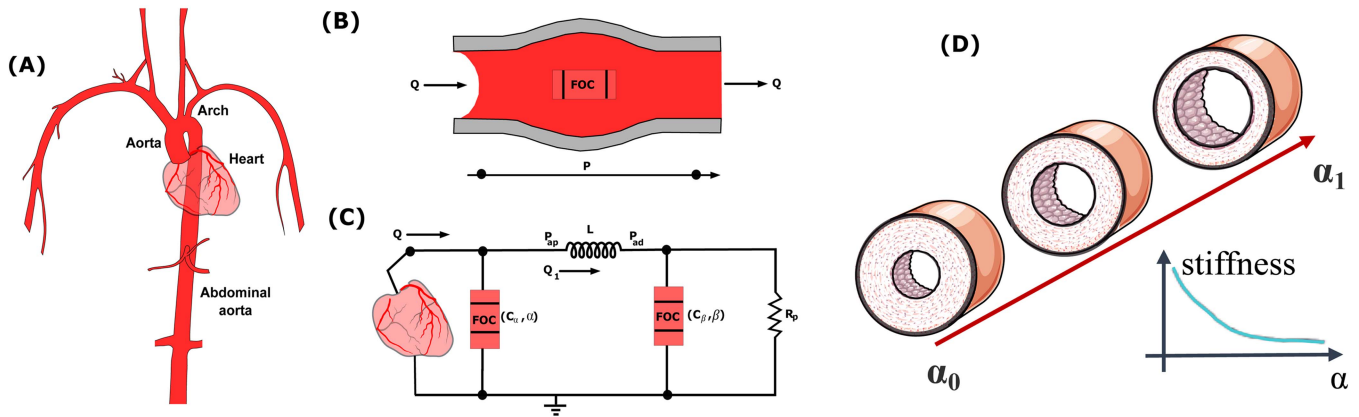
Fig. 1. Figure illustrates in a schematic manner the general framework for fractional-order modeling of the arterial system. (a): A schematic that shows a simplified left ventricle-aortic-arteries sub-domains; (b): A fractional-order model of the apparent arterial compliance using a fractional-order capacitor; (c): The Fractional-order modified Windkessel (F-MWK) model; and (d): Finally an illustration of the fractional differentiation order as a marker of the arterial stiffness.

to the transfer function between the blood volume (V) and input blood pressure (P_{in}). Here, we present its mathematical derivation. Based on the conservation mass, the arterial blood flow pumped from the heart to the vascular bed (Q_{in}) which can be written as:

$$Q_{in} = Q_{stored} + Q_{out}, \tag{1}$$

where Q_{stored} is the blood stored in the arterial tree, and Q_{out} corresponds to the flow out of the arterial system. In the frequency domain Q_{out} can be expressed as:

$$Q_{out}(w) = \frac{1}{R_{app}(\omega)} P_\omega(w). \tag{2}$$

where ω corresponds to the angular frequency and R_{app} is the apparent arterial resistance [2]. Q_{stored} is defined as the rate of flow by taking the first derivative of the volume equation for the time.

$$Q_{stored}(t) = \frac{dV}{dt} = \underbrace{\frac{dV(t)}{dP_{in}(t)}}_{C_{app}} \frac{dP_{in}(t)}{dt}, \tag{3}$$

Hence in the frequency domain Q_{stored} can be expressed as:

$$Q_{stored} = j\omega P_{in} C_{app} \tag{4}$$

Aortic input impedance Z_{in} defines the capacity of the vascular system to impede the blood rate dynamically. It corresponds to the left ventricular afterload. Functionally, it is expressed in the frequency domain as the ratio between the arterial blood pressure (P_{in}) and flow (Q_{in}) at the aortic level of the systemic vascular system that is:

$$Z_{in}(\omega) = \frac{P_{in}(\omega)}{Q_{in}(\omega)}, \tag{5}$$

Substituting (2) and (4) into (1) gives:

$$Q_{in} = j\omega P_{in} C_{app} + \frac{1}{R_{app}(\omega)} P_\omega(w). \tag{6}$$

Rearranging the above equation yields an expression for C_{app} in terms of Z_{in} and R_{app} as follow:

$$C_{app} = \frac{R_{app} - Z_{in}}{j\omega R_{app} Z_{in}} \tag{7}$$

B. Fractional-Order Capacitor

Fractional-order capacitor (FOC), known as the constant phase element [35], is a fractional-order electrical element representing the fractional-order derivative through its *curent-volatge* characteristic. In fact, the relationship between the current, $Q(t)$, passing through an FOC and the voltage, $P(t)$, across it with respect to time, t, can be written as follow:
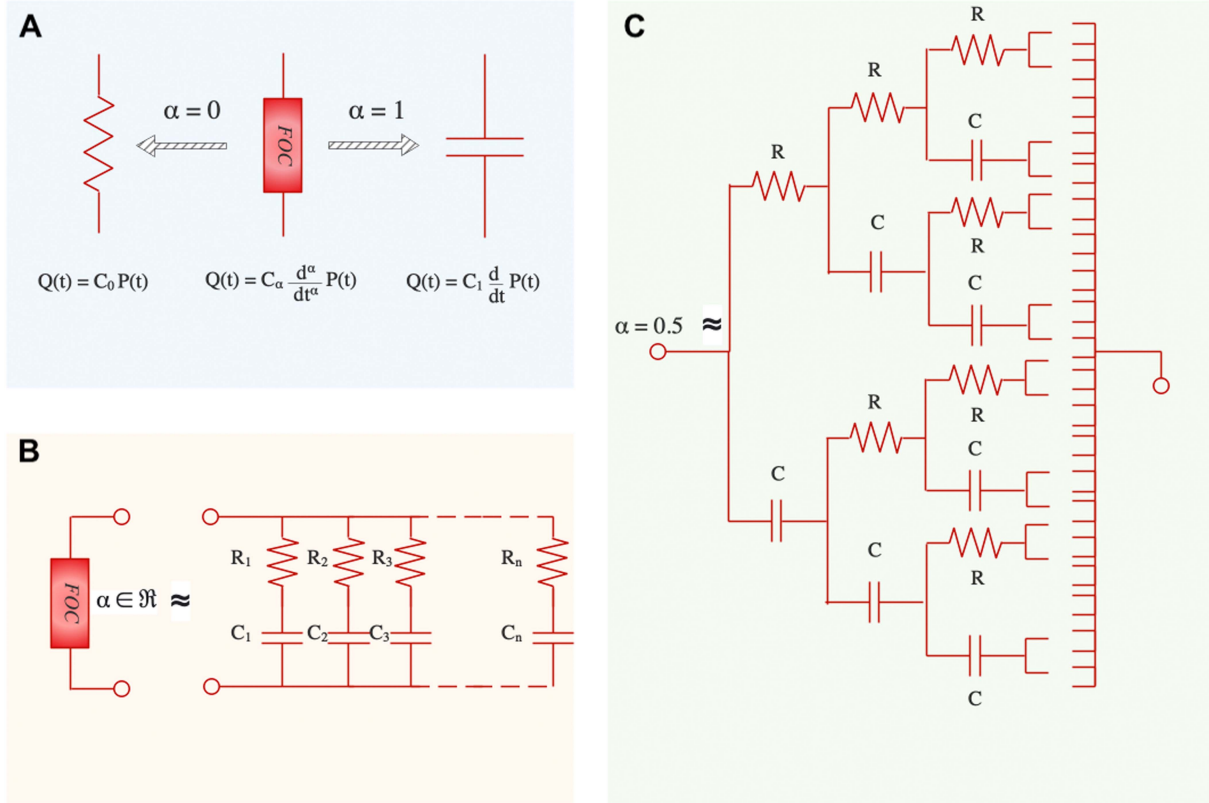
$$Q(t) = C_\alpha \frac{d^\alpha}{dt^\alpha} P(t), \tag{8}$$

where C_α is a proportionality constant so-called pseudo-capacitance, expressed in units of $[\text{Farad}/\text{second}^{1-\alpha}]$, [36]. The conventional capacitance, C, in unit of Farad is related to C_α as $C = C_\alpha \omega^{\alpha-1}$ that is frequency-dependent. The fractional-order impedance (Z_α) is expressed as follow:

$$Z_\alpha(s) = \frac{1}{C_\alpha s^\alpha} = \underbrace{\frac{1}{C_\alpha} \omega^{-\alpha} \cos(\phi)}_{Z_r} - j \underbrace{\frac{1}{C_\alpha} \omega^\alpha \sin(\phi)}_{Z_i}, \tag{9}$$

where s corresponds to the *Laplace* variable and ϕ denotes the phase shift expressed as: $\phi = \alpha\pi/2$ [rad] or $\phi = 90\alpha$ [degree or °]. Z_r and Z_i are the real and imaginary parts of Z_α corresponding to the resistive and capacitive portions, respectively. From (9), it is apparent that the transition between resistive and capacitive parts is ensured by α. If $0 \leq \alpha \leqslant 1$, the bounding conditions of α will correspond to the discrete conventional elements: the resistor at $\alpha = 0$ and the ideal capacitor at $\alpha = 1$. As α goes to 0, (Z_i) convergence to 0, and thus the fractional element looks like that of a pure resistor, whereas as α goes to 1, (Z_r) converges to 0 and hence, the fractional element serves as a pure capacitor, [37]. Fig. 2(a). represents the schematic diagram for a FOC, along with the ideal resistor and capacitor. Many studies have shown that FOC is equivalent to a resistor ladder network (RC tree circuit), [38], [39]. This structure is similar to

Fig. 2. (a) Circuit diagram of the ordinary resistor and capacitor and the constant phase element is (fractional-order capacitor). It also shows the *current-voltage* relationship (*Q-P*): fractional-order capacitor; $Q(t) = C_\alpha(d^\alpha/dt^\alpha)P(t)$ where $0 \leq \alpha \leq 1$ and C_α is the pseudo-capacitance. The limit values of α, namely for $\alpha = 0$ and $\alpha = 1$, correspond to the ordinary elements of the ideal resistor and capacitor, respectively. (b) Circuit diagram representing the equivalent RC tree circuit of the fractional-order capacitor of any order, $0 < \alpha < 1$. (c) Circuit diagram representing the equivalent RC tree circuit of the fractional-order capacitor when $\alpha = 0.5$.

the electrical analogy of the generalized Kelvin–Voigt viscoelastic model. Fig. 2(b). presents the equivalent RC tree circuit of FOC of any order, and Fig. 2(c). shows the equivalent RC tree circuit of FOC of order 0.5. Bearing these properties in mind, the fractional-order α parameter allows extra versatility in modeling viscoelastic systems [40]. As shown in the previous section, the FOC offers extra flexibility via its fractional differentiation order α, and it permits the smooth transition and control between the resistive and capacitive parts, which might be investigated to model the arterial system properties. By rewriting (3) in the fractional-order domain as:

$$Q_{stored}(t) = \frac{d^\alpha V}{dt^\alpha} = \underbrace{\frac{d^\alpha V(t)}{d^\alpha P_{in}(t)}}_{C_{\alpha_{app}}} \frac{d^\alpha P_{in}(t)}{dt^\alpha}. \qquad (10)$$

The FOC can be an inherent lumped element that can catch vascular compliance's complex and frequency-dependent behavior. In fact, as expressed in (10), the pseudo compliance, $C_{\alpha_{app}}$, should be expressed in the unit of $[\text{l/mmHg} \cdot \text{sec}^{1-\alpha}]$ that makes, naturally, the standard compliance (C_C), in the unit of $[\text{l/mmHg}]$, frequency-dependent as:

$$C_C = C_{\alpha_{app}}(j\omega)^{\alpha-1}. \qquad (11)$$

Hence the fractional-order capacitor presents physical bases in portraying the complex and frequency dependency of the

apparent vascular compliance. Besides, based on the variation of the fractional differentiation order α, the real and imaginary parts of the resultant FOC's impedance can possess various levels, so by analogy, α can control dissipative and storage mechanisms and hence the viscous and elastic component of the arterial wall. Furthermore, it is worth remarking that the equivalent circuit representation of FOC can be seen as an infinity of Voigt cells branches joined in parallel. Consequently, FOC simplifies the representation of the complex arterial network's mechanical properties by employing only two parameters (α and C_α). In the following, we present the five fractional-order representations of arterial compliance shown in Fig. 2. In addition, as in this study, the proposed models were compared with generalized ordinary (integer-order) vascular compliance models; we also present their expressions following the fractional-order ones.
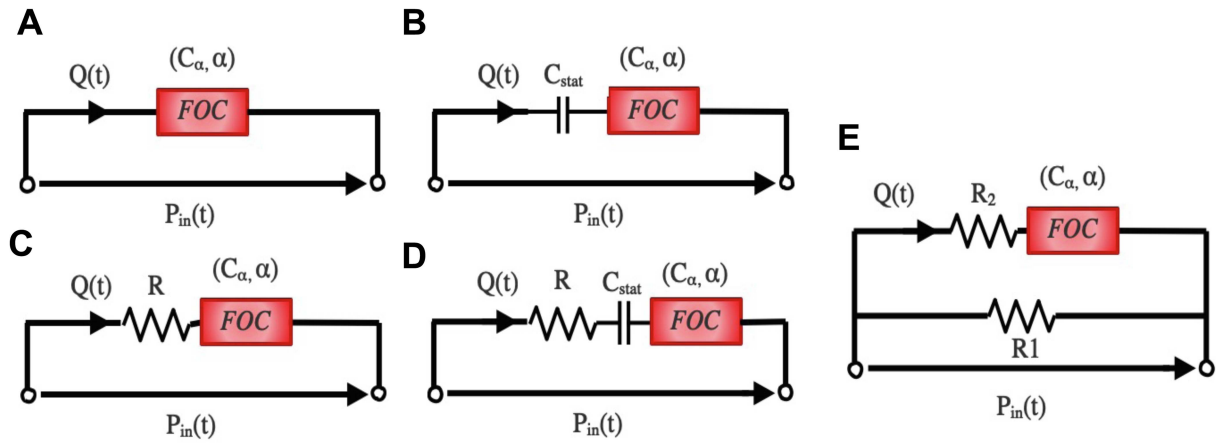
III. MODELS

A. Fractional-Order Models

Model A: As shown in Fig. 3(a), this representation consists of a single fractional-order capacitor. Accordingly, as mentioned previously, the apparent arterial compliance formulated in the unit of $[\text{l/mmHg}]$ can be expressed as follows:

$$C_{app}^A = C_\alpha(j\omega)^{\alpha-1}. \qquad (12)$$

Fig. 3. Figure illustrates in a schematic manner five representations of the proposed fractional-order apparent compliance models. All structures use fractional-order capacitor element that combines the complex and frequency-dependence characteristics of arterial compliance. The FOC modeling approach accounted for both resistive and capacitive properties.

Model B: As shown in Fig. 3(b), this representation consists of an ideal integer-order capacitor (C_{stat}) accounting for the static compliance connected in series to and FOC. The apparent arterial compliance formulated in the unit of $[l/mmHg]$ can be expressed as follows:

$$C_{app}^B = \frac{C_\alpha C_{stat}(j\omega)^\alpha}{C_\alpha(j\omega)^\alpha + C_{stat}(j\omega)}. \tag{13}$$

Model C: As shown in Fig. 3(c), this representation consists of an ideal resistor (R) connected in series to FOC. The apparent arterial compliance formulated in the unit of $[l/mmHg]$ can be expressed as follows:

$$C_{app}^C = \frac{C_\alpha(j\omega)^{\alpha-1}}{1 + RC_\alpha(j\omega)}. \tag{14}$$

Model D: As shown in Fig. 3(d), this representation consists of an ideal resistor (R), an ideal integer-order capacitor (C_{stat}), and FOC, all connected in series. The apparent arterial compliance formulated in the unit of $[l/mmHg]$ can be expressed as follows:

$$C_{app}^D = \frac{C_{stat}C_\alpha(j\omega)^\alpha}{C_{stat}(j\omega) + C_\alpha(j\omega)^\alpha + RC_\alpha C_{stat}(j\omega)^{\alpha+1}}. \tag{15}$$

Model E: As shown in Fig. 3(e), this representation consists of an ideal resistor (R_1) connected in parallel to a branch of a FOC in series with an ideal resistor (R_2). The apparent arterial compliance formulated in the unit of $[l/mmHg]$ can be expressed as follows:

$$C_{app}^E = \frac{1 + (R_1 + R_2)C_\alpha(j\omega)^{\alpha-1}}{R_1(1 + R_2C_\alpha(j\omega)^\alpha)}. \tag{16}$$

B. Integer-Order Models

Model F: This model expresses the apparent compliance based on the general viscoelastic model [41]. It is formulated

as follows:

$$C_{app}^F = C_{stat}\frac{\prod_{n=1}^N a_n(j\omega + b_n)}{\prod_{n=1}^N b_n(j\omega + a_n)}, \tag{17}$$

where a_n and b_n correspond to imperial constants that can be adapted to fit any special case. C_{stat} expresses the static compliance. Goedhard et al.l pointed out that this model could fit real experimental data with $N = 4$, which we adopt in our comparative study.

Model G: It corresponds to the Voigt-cell based-representation. It consists of an integer-order, ideal capacitor (C_{stat}) accounting for the static compliance in series to a resistor (R_d), accounting for viscous losses.

$$C_{app}^G = C_{stat}\frac{1}{1 + (j\omega)R_d C_{stat}} \tag{18}$$

IV. METHOD & MATERIAL

A. in-vivo Human Dataset

In order to validate the proposed approach, in this study, we use real data for human aging. The in-vivo human data was extracted and digitized from aging studies (Nichols et al., [42], [43]). The data consists of measured aortic blood flow rate (Q_a) and aortic blood pressure (P_a) at various ages, specifically 28, 52, and 68 years whose cardiac cycle is $T = 0.95$ Sec.

B. Parameters Fitting of the Models

To fully identify the proposed fractional-order model and the integer-order-based apparent compliance representations, the parameters, and the fractional differentiation orders have to be estimated using the measured flow and pressure waveforms. The estimation process was based on a non-linear least square minimization routine applying the well-known $MATLAB - R2020b$, the function *fmincon*. Regarding the stopping criteria for the optimizer, we have imposed a fixed final number of iterations that was selected based on a trial

---

Algorithm 1: Parameter Calibration of the Models.

1: Load the datasets of the aortic blood pressure (P_{in}) and flow rate (Q)
2: Evaluate the Fast Fourier Transform (FFT) of both P and Q
3: Select the frequency range (Hz) f $\in$ [0 12]
4: Calculate the aortic input impedance Z_{in} $\triangleright$ Using (5)
5: Calculate the in-silico apparent compliance C_{app} $\triangleright$ Using (7)
6: Select the model to fit with the data
7: Include and Initialize the parameter to estimate Θ
8: Solve the optimization problem

$$\hat{\Theta} = \arg \min_{\Theta} \ RMSE \tag{19}$$

$$RMSE = \sqrt{\frac{\sum_{i=1}^{N_s} \left(\left[\frac{Re - \hat{Re}}{\max(Re)} \right]^2 + \left[\frac{Im - \hat{Im}}{\max(Im)} \right]^2 \right)}{N_s}} \tag{20}$$

Where N_s denoting the number of explored frequency samples, Re and Im denoting the real and imaginary parts of the exprmental C_{app}, and Im, evaluated in step (5), and $\hat{Re}$ and $\hat{Im}$ corresponds to the real and imaginary parts of $C_{app}^{Model}(\Theta)$, respectively. $\hat{\theta}$ denotes the estimates that minimize $RMSE$

---

and error process so that it is enough to allow convergence of the optimization. The parameters to estimate for each model's representation C_c^{Model} are refereed as Θ^{Model} where $Model = \{(A), (B), (C), (D), (E), (F), (G)\}$ denotes to the index of the model's structure.

$$\Theta^{Model} = \begin{cases} C_{\alpha_A}, \alpha_A & \text{if } Model = A \\ C_{stat_B}, C_{\alpha_B}, \alpha_B & \text{if } Model = B \\ R_C; C_{\alpha_C}, \alpha_C & \text{if } Model = C \\ R_D; C_{stat_D}, C_{\alpha_D}, \alpha_D & \text{if } Model = D \\ R_{1_E}; R_{2_E}, C_{\alpha_E}, \alpha_E & \text{if } Model = E \\ C_{stat_F}, a_i |_{i=1,2,3,4}, b_i |_{i=1,2,3,4} & \text{if } Model = F \\ R_d; C_{stat} & \text{if } Model = G \end{cases}$$

Algorithm 1 summarizes the different steps applied to identify the different representations and estimate the model's parameters.

To analyze the ability of the developed models to reproduce the apparent arterial compliance dynamic, we evaluate the $RMSE$. In addition, because the model representations possess various numbers of parameters, to conduct a legitimate measurement and comparison, in addition to the $RMSE$, we assess the *Corrected Akaike Information Criterion* (AIC_C):

$$AIC_c = -2 \cdot ln(RMSE) + \frac{2 \cdot P \cdot N_s}{N_s - P - 1}. \tag{21}$$

where, P corresponds to the number of parameters and $RMSE$ is defined in (20).

V. RESULTS & DISCUSSION

A. Model Calibration

The evaluated *RMSE* and AIC_c, values after applying the proposed model and integer-order ones to the in-vivo human-aging data, are presented in Table I. Analyzing these results reveals that the fractional-order model representations grant an acceptable reproducing of the real arterial apparent compliance with a minimum number of parameters. Generally, the comparison between the proposed fractional-order models and the integer ones, namely Model (F) and (G), confirms that as the models differ in terms of performance, there is a trade-off between complexity induced by the number of parameters per representation and accuracy. Indeed, high-order models deliver high precision, however, at the expense of complexity. In order to take into account this compromise, the AIC_c has been evaluated.

For the 68 years old subject, *Model F* and *Model C* represent the lower error among the proposed fractional-order models and thus a better fit of the modulus and phase of the apparent arterial compliance. Although the integer-order model represents the lowest $RMSE$, it is complex as it requires nine parameters to be identified. This can be observed by analyzing the corrected Akaike Information Criterion (AIC_c), which is considered very high in all the studied subjects. The difference between the values of AIC_c of *Model F* and any other models is more than -2. Hence, the fractional-order representations can be considered significantly better than this model. It is worth noticing here that in this article, we present only the AIC_c. Still, in our analysis, we have calculated the *Bayesian Information Criteria (BIC)* and the *Akaike's Information Criteria (AIC)*. However, as the number of the studied samples is extremely small, we adopt the AIC_c. In fact, AIC_c is advocated when the sample size is relatively low.

For the 52 years old and 28 a old subjects *Model F Model C* and *Model C* represent the lower error among the proposed fractional-order models. Their $RMSE$ values are lower than the one of the integer-order *Model G* that represents the conventional Kelvin-Voigt model. For all the subjects, by examining the AIC_c values of all the models and evaluating the difference between AIC_C values of two models being compared, we can approve that: *Model A* can be considered as a reasonable candidate in describing the complex and frequency-dependent behavior of the apparent arterial compliance. Table II. presents the estimates of the unknown parameters of each fractional-order representation for each human and animal subject. Using *Model (A)* and *Model (B)*, for all the subjects, the fractional-order, α, is less than 1. These results demonstrate the fractional-order behavior within the apparent compliance. As in the estimation process, the estimate of α was only constrained to be positive, larger than zero (the lower bound is set to be 0 or the upper bound left unconstrained, equal to infinity). Therefore, this effect intends that the vascular system presents a viscoelastic behavior, not a purely elastic one. Actually, the fact that $\alpha \neq 1$ means that the fractional-order component involves both resistance and capacitance parts, as demonstrated mathematically in (9). The contributions from both the resistive and capacitive parts within the fractional-order capacitor are controlled through the

TABLE I
$RMSE$ & AIC_C CALCULATED BASED ON THE DEVELOPED FRACTIONAL-ORDER REPRESENTATION AND STANDARD ONES FOR EACH SUBJECT

		Model (A)	Model (B)	Model (C)	Model (D)	Model (F)	Model (E)	Model (G)
$RMSE$	68-yr	1.64	1.63	1.51	1.54	1.42	1.16	1.55
	52-yr	1.4	1.38	1.16	1.18	1.1	1.07	1.21
	28-yr	5.44	5.29	2.85	3.96	2.36	2.85	4.31
AIC_C	68-yr	4.34	4.35	8.18	8.14	13.02	107.7	4.45
	52-yr	4.65	4.7	8.7	8.66	13.52	107.87	4.95
	28-yr	1.95	2	6.9	6.25	12	105.9	2.41

TABLE II
PARAMETER ESTIMATES OF THE FRACTIONAL-ORDER MODELS FOR EACH SUBJECT

	Model (A)		Model (B)		Model (C)			Model (D)			Model (E)			
Age	C_{α_A}	α_A	C_{stat_B}, C_{α_B}	α_B	R_C	C_{α_C}	α_C	R_D	C_{stat_D}, C_{α_D}	α_D	R_{1_E}	R_{2_E}	C_{α_E}	α_E
68-yr	2.93	0.2	3.45	0.18	0.14	0.44	1.36	0.12	1.27	1.43	1.8	320	4.41e-5	1.49
52-yr	3.85	0.34	5.14	0.27	0.08	0.85	1.29	0.07	2.1	1.43	0.88	179.42	2.37e-4	1.25
28-yr	7.88	0.35	10.65	0.27	0.04	0.92	1.63	0.04	4.36	1.47	0.43	57.17	5.47e-4	1.39

fractional-order, α, allowing a profound physiological characterization. As the α moves to 1, the capacitance component becomes predominant and, hence the vascular mechanism functions as a pure elastic system, and as α goes to 0, the resistive portion expands, and so the vascular mechanism operates as a pure viscous system. By examining the estimates of the fractional orders of *Models (C), (D)* and *(E)*, it is noticeable that for all the subjects, $\hat{\alpha}$ is higher than 1. Functionally, as α beats 1, the real part of the fractional-order capacitor impedance, Z_r, converts negative, and hence it has the characteristic of a negative resistor producing power. Having a negative resistance in these models appears as compensation for the added static resistance in those representations. It is worth mentioning that the interest of constant resistor and/or capacitor in these fractional-order models is to account for the static viscosity and/or elasticity, respectively, while the fractional-order capacitor represents the ability of the arterial vessel to store blood dynamically.

B. Physiological Consistency of the Fractional Differentiation Order Parameter

The fractional-order paradigm affords a concise alternative to characterize and quantify the biomechanical behavior of membranes, cells, and tissues. In fact, many studies have found that the fractional-order framework is particularly relevant in the area of biorheology characterization. This is because many tissue-like materials present power-law responses to applied stress or strain. The power-law response has also been observed within the viscoelastic characterization of the aorta. in-vivo and in-vitro experiments and analysis showed the convenience of using fractional order viscoelastic model rather than the integer-order ones [25]. As shown previously, fractional differential order provides extra flexibility to model the apparent arterial compliance. It appears that the changes in the composition of the viscoelasticity of the whole vascular system are conveniently described in the fractional differentiation order of the model system. Based on the model formulation, the fractional parameter is convenient for describing the transition between viscosity and elasticity levels. Although the lack of enough real data, we investigate the interpretability and physiological consistency of

the fractional differentiation order in this part. By checking the values of the fractional differentiation order estimates, it is clear that α_A and α_B increase as the age decreases. This result is in coherence with what has been demonstrated in several human-aging studies. In fact, it is well recognized that the arterial vessel becomes stiffer with age [44]. Moreover, vascular stiffening provokes an increase in arterial pulse pressure, which deeply affects the blood vessels and heart functions. Physical stiffening of the arteries is recognized as the structural determinant of vascular aging. On the other hand, as we explained before when α goes to 0, the resistive part increases within the fractional-order element, and the system behaves as a viscous element. For the other models based $\{\alpha_C, \alpha_D,$ and $\alpha_E\}$ where their values exceed 1, we can notice that from 68 years old subject to 52 years old one, the values of α decrease; however, the 28 years old subject presents the highest value.

The analysis of the variation of the fractional differentiation order and its association with different ages points out the potential of this parameter to be adopted as a surrogate measure of the arterial stiffness or marker of cardiovascular diseases. Future clinical and experimental validations are required to prove the concept within a wide spectrum of normal and pathological cardiovascular conditions. To show the added value of the fractional-order element and its interaction with other compartments in a global arterial representation, in the following, we present a fractional-order arterial Windkessel model. The developed model includes the simplest fractional-order structure *Model A* of the apparent arterial compliance to take into account the effect of the proximal and distal compliance.

VI. EXAMPLE OF ARTERIAL WINDKESSEL MODEL USING FRACTIONAL-ORDER COMPLIANCE

In order to evaluate the effect of integration of the proposed fractional-order compliance representations within a complete arterial lumped parameter model, in this section, we present a fractional-order Modified Windkessel model based on a fractional-order capacitor. We validate the output pressure waveforms through the forward fractional-order framework.

Age	Parameters estimates						Performance		
	C_α	L	C_β	R_p	α	β	$P-RMSE$	$R.E.(\%)$	ρ
68-years	0.72	0.00013	0.73	2.00	1.00	0.43	3.51	3.26	0.98
52-years	1.51	0.03600	1.05	1.86	1.03	0.46	2.29	2.33	0.99
28-years	8.94	0.01200	2.00	0.16	1.09	0.85	1.52	1.67	0.99

A. Fractional-Order Modified Windkessel Model

The modified Windkessel model (MWK) is one of the simplest arterial representations that lumps the arterial network into two main compartments, proximal and distal, [45]. Taking into account that the proximal arteries close to the heart have different properties in comparison to the distal ones, MWK splits the total arterial compliance used in the original arterial Windkessel into two capacitances: proximal capacitor represents the compliance of the large arteries, which are commonly elastic and distal capacitor depicts the compliance of muscular arteries that are stiffer. Clinical studies demonstrated that distal compliance is very sensitive to vasodilatory experiments, a property apparent in distal arteries. Other investigations have also shown that proximal compliance is reduced with aging and hypertension. The latest properties make these capacitances potential indicators of cardiovascular risk.

Fig. 1(c) shows the circuit model of the fractional-order modified arterial Windkessel (F-MWK), which is similar to the MWK; however, instead of using integer-order ideal capacitors to represent the arterial compliances, simple fractional-order capacitors are employed. In this arterial lumped model, C_α represents the compliance of large arteries close to the heart, while C_β represents that of muscular arteries further away from the heart. L represents the inertance of the flowing blood. R_p represents the peripheral resistance. $Q(t)$ corresponds to the arterial blood flow and $P_{ap}(t)$ and $P_{ad}(t)$ denotes the proximal and distal pressure respectively.

B. F-MWK Mathematical Model

As the model comprises two fractional-order capacitors and an inductor, a state space representation with three states are written to describe the dynamic of the arterial system. Based on Kirchhoff's voltage and current laws, we obtain the following three equations:

$$D_t^q x(t) = Ax(t) + u(t), \qquad (22)$$

where,

$$D_t^q = \left[\frac{d^\alpha}{dt^\alpha}, \frac{d^1}{dt^1}, \frac{d^\beta}{dt^\beta} \right]^{tr} \qquad (23)$$

is the fractional-order derivative operator for all the states and

$$x(t) = [P_{ap}(t), Q_1(t), P_{ad}(t)]^{tr} \qquad (24)$$

represents the state vector, $(\cdot)^{tr}$ denotes the transpose of the row vector. A represents the parameters and is expressed as:

$$A = \begin{bmatrix} 0 & -\dfrac{1}{C_\alpha} & 0 \\ \dfrac{1}{L} & 0 & -\dfrac{1}{L} \\ 0 & \dfrac{1}{C_\beta} & -\dfrac{1}{R_p C_\beta} \end{bmatrix} \qquad (25)$$

$$u(t) = \left[\frac{Q(t)}{C_{ap}}\ 0\ 0 \right]^{tr} \qquad (26)$$

To implement the fractional-order derivative we used the following *Grünwald–Letnikov* (GL) formula [46], [47]:

$$\frac{d^\alpha}{dt^\alpha} f(t) = \lim_{h\to 0} \frac{1}{h^\alpha} \sum_{i=0}^{\infty} c_i^{(\alpha)} f(t - ih), \quad \alpha > 0, \qquad (27)$$

where $h > 0$ is the time step, $c_i^{(\alpha)}$ $(i = 0, 1, \ldots)$ are the binomial coefficients recursively computed using the following formula,

$$c_0^{(\alpha)} = 1, \ c_i^{(\alpha)} = \left(1 - \frac{1+\alpha}{i} \right) c_{i-1}^{(\alpha)}. \qquad (28)$$

C. Validation

The time validation of the proximal pressure waveforms P_{ap} was performed through the proposed F-MWK using the in-vivo human-aging database described in Section IV-A. The optimizer algorithm uses the measured aortic root flow rate as input and computes the required model parameters, $\{C_\alpha, L, C_\beta, R_p, \alpha, \beta\}$, which minimize the pressure root mean square error (P-RMS), i.e., the difference between measured and calculated aortic root pressure as:

$$P-RMSE = \sqrt{\frac{1}{N} \Sigma_{i=1}^{n} (P_{ap_i} - \hat{P}_{ap_i})^2} \qquad (29)$$

Where N denotes the number of samples per P_{ap} pressure signal. To evaluate the performance of the estimation, we calculate the relative error, $R.E.(\%)$ and the correlation coefficient, ρ defined as:

$$\begin{cases} R.E.(\%) = \dfrac{||P_{ap} - \hat{P}_{ap}||_2}{||P_{ap}||_2} \times 100\% \\[4mm] \rho = \dfrac{\sum_{i=1}^{n} (P_{ap} - \bar{P}_{ap})(\hat{P}_{ap} - \bar{\hat{P}}_{ap})}{\sqrt{\sum_{i=1}^{n}(P_{ap} - \bar{P}_{ap})^2} \sqrt{\sum_{i=1}^{n}(\hat{P}_{ap} - \bar{\hat{P}}_{ap})^2}}, \end{cases} \qquad (30)$$

where $\bar{\ }$ represents the average operator.

Table III summarizes the parameter estimates of the proposed F-MWK for each age. It also shows the results of the root
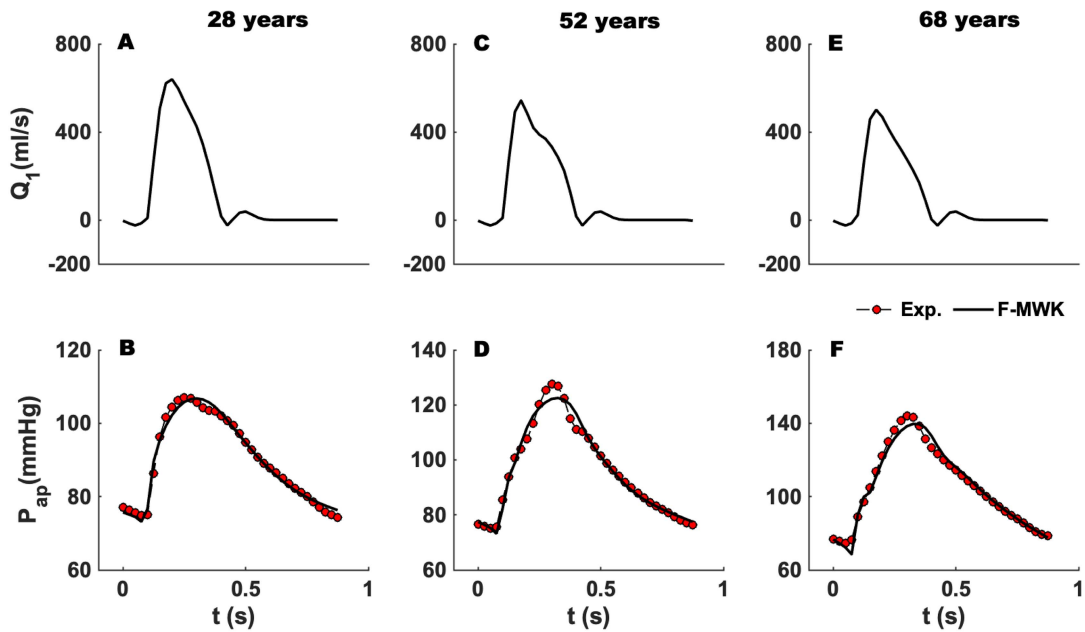
Fig. 4. Estimated proximal blood pressure using the proposed fractional-order modified Windkessel model along with the experimental in-vivo human-aging. A, C, and E represent the model input aortic-valve blood flow rate for each validation case of study, 28, 52, and 68 years old, respectively. B, D, and F represent The pressure waveform validation results.
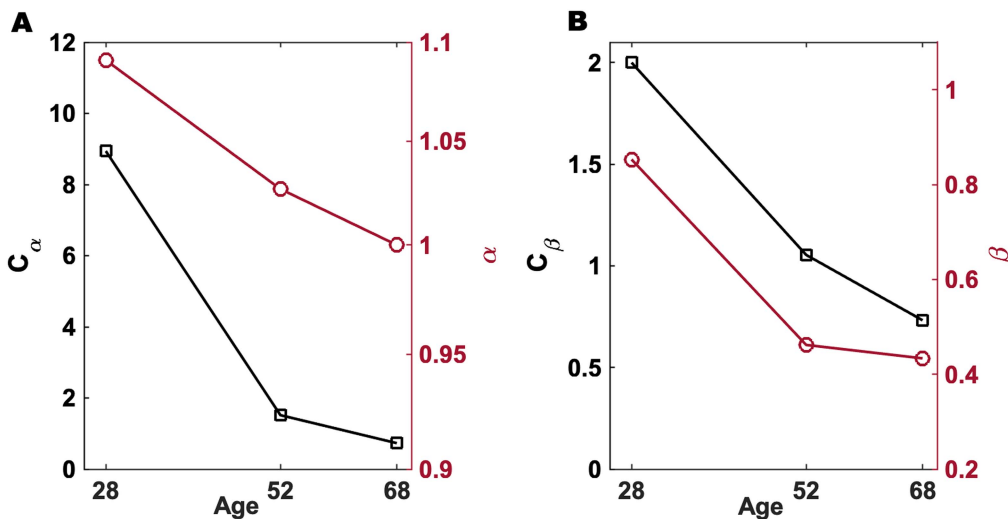
Fig. 5. (a) Pseudo-capacitance estimate of the proximal compliance C_α left y-axis and Fractional differentiation order estimates, α, of the proximal compliance right y-axis, (b) Pseudo-capacitance estimate of the distal compliance C_β, left y-axis and Fractional differentiation order estimates, β, of the distal compliance right y-axis.

mean square error ($P-EMSE$), the relative errors ($R.E.(\%)$), and the correlation coefficient (ρ) of the estimated aortic blood pressure values for each subject. Fig. 4 shows the reconstructed blood pressure using the proposed F-MWK model along with the measured in-vivo blood waveform for each case of study, namely, 28, 52, and 68 years. The proposed model is able to reconstruct the aortic blood pressure and capture the main features during the different phases of the cardiac cycle (systolic and diastolic phases).

Arterial compliance is an important measure of cardiovascular function, and it is determined by the ability of blood vessels to expand and contract in response to changes in blood pressure. In this study, we examined the fractional differentiation orders (α, β) and pseudo-capacitances (C_α, C_β) of the proximal and distal compliances of three subjects, as shown in Fig. 5. These parameters provide a quantitative measure of arterial compliance, and they are often used to assess changes in arterial function with age. Our results indicate that there is a negative correlation

between age and arterial compliance. Specifically, as individuals age, the values of α and β decrease, indicating a reduction in the compliant part of arterial function. Similarly, the values of C_α and C_β also decrease with age, which suggests a reduction in the capacity of the blood vessels to store energy. These findings are consistent with previous clinical studies that have shown that arterial compliance decreases with age. The decrease in arterial compliance is thought to be due to a combination of factors, including changes in the structural and mechanical properties of the arterial wall, alterations in the composition of the extracellular matrix, and changes in the function of smooth muscle cells and endothelial cells. In particular, the decrease in arterial compliance that we observed is indicative of an increase in the resistive part of arterial function. This suggests that blood vessels become stiffer and less able to accommodate changes in blood pressure as individuals age. This is a concerning finding, as decreased arterial compliance has been associated with an increased risk of cardiovascular disease, including hypertension, stroke, and heart attack. Overall, our results provide important insights into the mechanisms underlying age-related changes in arterial function and highlight the need for interventions to promote healthy aging and prevent the development of cardiovascular disease. Future research should focus on identifying the specific factors that contribute to the decrease in arterial compliance with age and developing targeted interventions to address theset factors.

VII. Conclusion

Arterial compliance is a vital determinant of the ventriculo-arterial coupling dynamic. Its variation is detrimental to cardiovascular functions and is associated with heart diseases. Accordingly, assessment and measurement of arterial compliance are essential in diagnosing and treating chronic arterial insufficiency. Indices and surrogate measurements of arterial compliance present a non-invasive assessment of the vasculature's health and can provide appropriate knowledge about an individual's future risk of morbidity and mortality. The fractional-order behavior by means of the power-low response has been shown in the characterization of the collagenous tissues in the arterial bed, the arterial hemodynamic, the red blood cell membrane mechanics, and the heart valve cusp. This paper investigates the fractional-order framework to characterize vascular compliance. Accordingly, we introduce five fractional-order lumped parametric representations to assess apparent arterial compliance. The proposed models vary in terms of the number of elements to characterize compliance's dynamic. Every configuration contains a fractional-order capacitor (FOC) that accounts for the complex and frequency-dependence characteristics of the compliance. FOC lumps both viscous and elastic properties of the vascular wall in one component, controlled through the fractional differentiation order (α) of FOC. To fully identify the proposed models, the unknown parameters and the fractional differentiation order were estimated using real hemodynamic data collected from human aging subjects. The developed parametric models produce an accurate reconstruction of the real data.

In order to verify the proposed concepts within a global arterial pattern, A novel fractional-order modified arterial Windkessel model that incorporates a fractional-order FOC element was proposed to capture the complex and frequency-dependent properties of proximal and distal compliances. The results using real human aortic blood pressure and flow data show a good reconstruction of the proximal blood pressure. In addition, the values of the compliances and their fractional differentiation orders were in agreement with the clinical results of the aging implications. Conclusively, our investigation attests that the fractional-order modeling framework conveniently captures the dynamic capacity of the vascular system to store blood. In addition, it shows that the fractional-order paradigm has a prominent potential to afford an alternative to assessing arterial stiffness.

In future work, it is imperative to procure an expanded dataset of human aging data to substantiate the viability of our proposed proof of concept. Additionally, we intend to conduct an exhaustive investigation into the influence of specific cardiovascular pathologies on variations in dynamic arterial compliance, elucidated through the utilization of the fractional-order capacitor model. The incorporation of this supplementary data and analysis is anticipated to augment the overall comprehensiveness and robustness of our scientific study.

References

[1] Y. Ruan et al., "Cardiovascular disease (CVD) and associated risk factors among older adults in six low-and middle-income countries: Results from SAGE wave 1," *BMC Public Health*, vol. 18, no. 1, pp. 1–13, 2018.

[2] C. M. Quick, D. S. Berger, and A. Noordergraaf, "Apparent arterial compliance," *Amer. J. Physiol.-Heart Circulatory Physiol.*, vol. 274, no. 4, pp. H1393–H1403, 1998.

[3] M. Bahloul, "Contributions to data-driven and fractional-order model-based approaches for arterial haemodynamics characterization and aortic stiffness estimation," Ph.D. dissertation, King Abdullah Univ. Sci. Technol., Saudi Arabia, 2022.

[4] I. Mackenzie, I. Wilkinson, and J. Cockcroft, "Assessment of arterial stiffness in clinical practice," *Qjm*, vol. 95, no. 2, pp. 67–74, 2002.

[5] M. Bahloul, Z. Belkhatir, Y. Aboelkassem, and M. T. Laleg-Kirati, "Physics-based modeling and data-driven algorithm for prediction and diagnosis of atherosclerosis," *Biophysical J.*, vol. 121, no. 3, pp. 419a–420a, 2022.

[6] B. Haluska, L. Jeffriess, J. Brown, S. Carlier, and T. Marwick, "A comparison of methods for assessing total arterial compliance," *J. Hum. Hypertension*, vol. 24, no. 4, pp. 254–262, 2010.

[7] D. Valdez-Jasso, D. Bia, Y. Zócalo, R. L. Armentano, M. A. Haider, and M. S. Olufsen, "Linear and nonlinear viscoelastic modeling of aorta and carotid pressure–area dynamics under in vivo and ex vivo conditions," *Ann. Biomed. Eng.*, vol. 39, no. 5, pp. 1438–1456, 2011.

[8] N. Stergiopulos, P. Segers, and N. Westerhof, "Use of pulse pressure method for estimating total arterial compliance in vivo," *Amer. J. Physiol.-Heart Circulatory Physiol.*, vol. 276, no. 2, pp. H424–H428, 1999.

[9] N. Westerhof, J.-W. Lankhaar, and B. E. Westerhof, "The arterial windkessel," *Med. Biol. Eng. Comput.*, vol. 47, no. 2, pp. 131–141, 2009.

[10] P. Segers et al., "Pulse pressure method and the area method for the estimation of total arterial compliance in dogs: Sensitivity to wave reflection intensity," *Ann. Biomed. Eng.*, vol. 27, no. 4, pp. 480–485, 1999.

[11] G. d. Simone, M. J. Roman, M. J. Koren, G. A. Mensah, A. Ganau, and R. B. Devereux, "Stroke volume/pulse pressure ratio and cardiovascular risk in arterial hypertension," *Hypertension*, vol. 33, no. 3, pp. 800–805, 1999.

[12] D. Chemla et al., "Total arterial compliance estimated by stroke volume-to-aortic pulse pressure ratio in humans," *Amer. J. Physiol.-Heart Circulatory Physiol.*, vol. 274, no. 2, pp. H500–H505, 1998.

[13] M. Kaya, V. Balasubramanian, A. Patel, Y. Ge, and J. K. Li, "A novel compliance-pressure loop approach to quantify arterial compliance in systole and in diastole," *Comput. Biol. Med.*, vol. 99, pp. 98–106, 2018.

[14] Y. Ge, "A new approach to assess arterial system function with compliance-pressure loop," Ph.D. dissertation, Rutgers Univ.-School of Graduate Studies, New Brunswick, NJ, USA, 2018.

[15] C. M. Quick, D. S. Berger, D. A. Hettrick, and A. Noordergraaf, "True arterial system compliance estimated from apparent arterial compliance," *Ann. Biomed. Eng.*, vol. 28, no. 3, pp. 291–301, 2000.

[16] D. Craiem and R. Armentano, "The new apparent compliance concept as a simple lumped model," *Cardiovasc. Engineering: Int. J.*, vol. 3, no. 2, pp. 81–83, 2003.

[17] R. Burattini and S. Natalucci, "Complex and frequency-dependent compliance of viscoelastic windkessel resolves contradictions in elastic windkessels," *Med. Eng. Phys.*, vol. 20, no. 7, pp. 502–514, 1998.

[18] R. Visaria, *Modeling of Cardiovascular System, Pulmonary Mechanics and Gas Exchange*. Salt Lake City, UT, USA: Univ. Utah, 2005.

[19] M. A. Bahloul, Y. Aboelkassem, and T.-M. Laleg-Kirati, "Human hypertension blood flow model using fractional calculus," *Front. Physiol.*, vol. 13, 2022, Art. no. 838593.

[20] Z. Belkhatir, F. Alhazmi, M. A. Bahloul, and T.-M. Laleg-Kirati, "Parameter sensitivity and experimental validation for fractional-order dynamical modeling of neurovascular coupling," *IEEE Open J. Eng. Med. Biol.*, vol. 3, pp. 69–77, 2022.

[21] M. A. Bahloul, A. Chahid, and T.-M. Laleg-Kirati, "Fractional-order SEIQRDP model for simulating the dynamics of COVID-19 epidemic," *IEEE Open J. Eng. Med. Biol.*, vol. 1, pp. 249–256, 2020.

[22] P. Perdikaris and G. E. Karniadakis, "Fractional-order viscoelasticity in one-dimensional blood flow models," *Ann. Biomed. Eng.*, vol. 42, no. 5, pp. 1012–1023, 2014.

[23] J. P. Zerpa, A. Canelas, B. Sensale, D. B. Santana, and R. Armentano, "Modeling the arterial wall mechanics using a novel high-order viscoelastic fractional element," *Appl. Math. Modelling*, vol. 39, no. 16, pp. 4767–4780, 2015.

[24] M. A. Bahloul and T.-M. Laleg-Kirati, "Assessment of fractional-order arterial windkessel as a model of aortic input impedance," *IEEE Open J. Eng. Med. Biol.*, vol. 1, pp. 123–132, 2020.

[25] D. Craiem and R. L. Magin, "Fractional order models of viscoelasticity as an alternative in the analysis of red blood cell (rbc) membrane mechanics," *Phys. Biol.*, vol. 7, no. 1, 2010, Art. no. 013001.

[26] T. C. Doehring, A. D. Freed, E. O. Carew, and I. Vesely, "Fractional order viscoelasticity of the aortic valve cusp: An alternative to quasilinear viscoelasticity," *J. biomechanical Eng.*, vol. 127, no. 4, pp. 700–708, 2005.

[27] D. Craiem and R. L. Armentano, "A fractional derivative model to describe arterial viscoelasticity," *Biorheology*, vol. 44, no. 4, pp. 251–263, 2007.

[28] D. Craiem, F. J. Rojo, J. M. Atienza, R. L. Armentano, and G. V. Guinea, "Fractional-order viscoelasticity applied to describe uniaxial stress relaxation of human arteries," *Phys. Med. Biol.*, vol. 53, no. 17, p. 4543, 2008.

[29] M. A. Bahloul and T.-M. Laleg-Kirati, "Three-element fractional-order viscoelastic arterial windkessel model," in *Proc. 40th Annu. Int. Conf. IEEE Eng. Med. Biol. Soc.*, 2018, pp. 5261–5266.

[30] M. A. Bahloul and T. M. Laleg-Kirati, "Arterial viscoelastic model using lumped parameter circuit with fractional-order capacitor," in *Proc. IEEE 61st Int. Midwest Symp. Circuits Syst.*, 2018, pp. 53–56.

[31] M. A. Bahloul and T.-M. L. Kirati, "Two-element fractional-order windkessel model to assess the arterial input impedance," in *Proc. 41st Annu. Int. Conf. IEEE Eng. Med. Biol. Soc.*, 2019, pp. 5018–5023.

[32] T. M. Laleg and M. A. Bahloul, "Mathematical biomarker for arterial viscoelasticity assessment," US Patent 20210353160A1, Nov. 18, 2021.

[33] M. A. Bahloul and T.-M. L. Kirati, "Fractional-order model representations of apparent vascular compliance as an alternative in the analysis of arterial stiffness: An in-silico study," *Physiol. Meas.*, vol. 42, no. 4, 2021, Art. no. 045008.

[34] M. Bahloul, Y. Aboelkassem, T.-M. Laleg, M. A. Bahloul, Y. Aboelkassem, and T.-M. L.-K. Team, "Fractional-order modeling of the complex and frequency-dependent arterial compliance: In human and animal validation," in *Proc. APS Division Fluid Dyn. Meeting Abstr.*, 2021, pp. T15–012.

[35] A. Kartci, N. Herencsar, J. T. Machado, and L. Brancik, "History and progress of fractional-order element passive emulators: A review," *Radio-engineering*, vol. 29, no. 2, Jun. 2020, doi: 10.13164/re.2020.0296.

[36] A. S. Elwakil, "Fractional-order circuits and systems: An emerging interdisciplinary research area," *IEEE Circuits Syst. Mag.*, vol. 10, no. 4, pp. 40–50, Fourthquarter 2010.

[37] M. S. Krishna, S. Das, K. Biswas, and B. Goswami, "Fabrication of a fractional order capacitor with desired specifications: A study on process identification and characterization," *IEEE Trans. Electron Devices*, vol. 58, no. 11, pp. 4067–4073, Nov. 2011.

[38] G. Carlson and C. Halijak,, "Approximation of fractional capacitors $(1/s)^{(1/n)}$ by a regular Newton process," *IEEE Trans. Circuit Theory*, vol. 11, no. 2, pp. 210–213, Jun. 1964.

[39] G. Si, L. Diao, J. Zhu, Y. Lei, and Y. Zhang, "Attempt to generalize fractional-order electric elements to complex-order ones," *Chin. Phys. B*, vol. 26, no. 6, 2017, Art. no. 060503.

[40] C. Vastarouchas and C. Psychalinos, "Biomedical and biological applications of fractional-order circuits," in *Proc. Panhellenic Conf. Electron. Telecommun.*, 2017, pp. 1–4.

[41] W. Goedhard and A. Knoop, "A model of the arterial wall," *J. Biomech.*, vol. 6, no. 3, pp. 281–288, 1973.

[42] W. W. Nichols, A. P. Avolio, R. P. Kelly, and M. F. Órouke, "Effect of age and of hypertension on wave travel and reflections," in *Arterial Vasodilation: Mechanisms and Therapy*, M. F. O'Rouke, Ed. London, U.K.: Edward Arnord, 1993, pp. 23–40.

[43] Y. Aboelkassem and Z. Virag, "A hybrid windkessel-womersley model for blood flow in arteries," *J. Theor. Biol.*, vol. 462, pp. 499–513, 2019.

[44] N. A. Shirwany and M.-H. Zou, "Arterial stiffness: A brief review," *Acta Pharmacologica Sinica*, vol. 31, no. 10, pp. 1267–1276, 2010.

[45] S. E. Francis, "Continuous estimation of cardiac output and arterial resistance from arterial blood pressure using a third-order windkessel model," Ph.D. dissertation, Massachusetts Inst. Technol., Cambridge, MA, USA, 2007.

[46] M. A. Bahloul and T.-M. L. Kirati, "Finite-time joint estimation of the arterial blood flow and the arterial windkessel parameters using modulating functions," *IFAC-PapersOnLine*, vol. 53, no. 2, pp. 16 286–16 292, 2020.

[47] M. A. Bahloul, M. Benencase, Z. Belkhatir, and T.-M. L. Kirati, "Finite-time simultaneous estimation of aortic blood flow and differentiation order for fractional-order arterial windkessel model calibration," *IFAC-PapersOnLine*, vol. 54, no. 15, pp. 538–543, 2021.